MEASUREMENT OF SKIN-FRICTION DRAG VARIATIONS BY ACTIVE TURBULENCE CONTROL USING A FIBER BRAGG GRATING SYSTEM

Takehiko Segawa, Yoshihiro Kikushima, Hiroyuki Abe, Hiro Yoshida
Institute for Energy Utilization,
National Institute of Advanced Industrial Science and Technology
1-2-1 Namiki, Tsukuba 305-8564, Japan
t-segawa@aist.go.jp, y.kikushima@aist.go.jp, abe.hiroyuki@aist.go.jp, h.yoshida@aist.go.jp

Koki Murakami, Hiroshi Mizunuma
Graduate School of Engineering,
Tokyo Metropolitan University
1-1 Minami-Osawa, Hachioji, Tokyo 192-0397, Japan
murakami-kouki@c.metro-u.ac.jp, mizunuma@ecomp.metro-u.ac.jp

ABSTRACT

A fiber Bragg grating (FBG) sensor system was developed to evaluate active flow-control devices. The FBG system was used for direct measurement of skin frictional drags in laminar and turbulent flows both in a water channel and a wind tunnel. Three FBG sensors were used: two for strain/drag measurements and one for monitoring temperature fluctuations. The FBG system could accurately observe minute skin friction variations of a wall, i.e. floating flat plate. Moreover, an appreciable drag reduction effect caused by a suction-blowing type actuator array was detected. This result indicates that the developed FBG system can be used to evaluate the performances of various flow control actuators under development.

INTRODUCTION

Near-wall streamwise vortices, such as low-speed streak structures, are known to be the main origin of turbulence production and increased drag. In the last decade, various strategies have been examined to control the near-wall vortex structures to reduce skin friction drags in the turbulent boundary layer (for example, Gad-el-Hak, 2000 and Choi, 2001a). Some strategies were incarnated by a passive method called riblets (Walsh and Lindemann, 1984, Choi, 1989, and Merigaud et al., 1996). Other strategies adopted active methods in which various control actuators were employed. Active control methods have been studied in many fields ranging from delaying of the transition to regulating the fully developed turbulent boundary layer. For example, Gad-el-Hak and Blackwelder (1989) and Myose and Blackwelder (1995) showed that a selective suction through a number of holes or slots in the wall delays the breakdown of the low-speed region and consequently reduces the production of turbulent energy in the turbulent boundary layer. Breuer et al. (1989) examined the interactions between low-speed coherent structures and artificial disturbances, which were produced by oscillating small membrane actuators vertically.

Recently, spanwise wall oscillation in a channel has been found to bring about considerable drag reduction. This finding supports the feasibility of active control of turbulence using actuators. Jung et al. (1992) performed a direct numerical simulation (DNS) on an oscillating wall in a turbulent channel flow. They predicted that wall oscillations in the spanwise direction could reduce the skin friction drags by 40%. They assumed that the drag reduction was brought about by viscous sub-layer thickening caused by the wall oscillation. These new findings of the numerical analysis by Jung et al. (1992) were supported by the experiments of Laadhari et al. (1994). They showed that the gradients of the mean velocity in the boundary layer were reduced near the oscillating wall and detected a slight reduction of the turbulent intensity across the boundary layer. This means that friction drags in the turbulent boundary layer can be reduced by wall oscillation. Local drag reduction caused by the spanwise wall oscillation was experimentally confirmed by Choi et al. (1998a) and Choi and Clayton (2001b). Furthermore, Choi and Graham (1998b) found that the skin friction drags were decreased by not only flat wall spanwise oscillation but also by circular-wall oscillation in turbulent pipe flows. They showed that an oscillating part of the pipe in a turbulent circular pipe flow produced a similar drag reduction effect with the flat wall oscillation. Thus, skin friction drag reduction caused by spanwise wall oscillation has been confirmed both analytically and experimentally.

However, oscillating an entire wall or a part of wall in an industrial application generally does not seem to be a realistic solution. The energy input for oscillating walls might be much greater than the gain from the resulting drag reduction. Current new technology on micro electro-mechanical systems (MEMS), which do not consume much power to drive the control system, is expected to offer the potential of controlling the near-wall turbulent structures. Several MEMS devices have been developed to sense and actuate near-wall coherent structures (for example, Kumar et al., 1999 and Kimura et al., 1999). The question we pose is how can we realize the same drag reduction effect as produced by wall oscillation by using intelligent MEMS devices with negligible energy consumption?

Extensive effort has also been made to elucidate the behavior of ordered or coherent motions in near-wall turbulence. One of the most profound findings regarding the cause of turbulent skin friction is that skin friction drags are mainly produced by so-called ejection and sweep (see Kline et al., 1967 and Corino and Brodkey, 1969). In the ejection, lower-speed clusters in the near-wall region rush into a higher speed region away from the wall. Conversely,

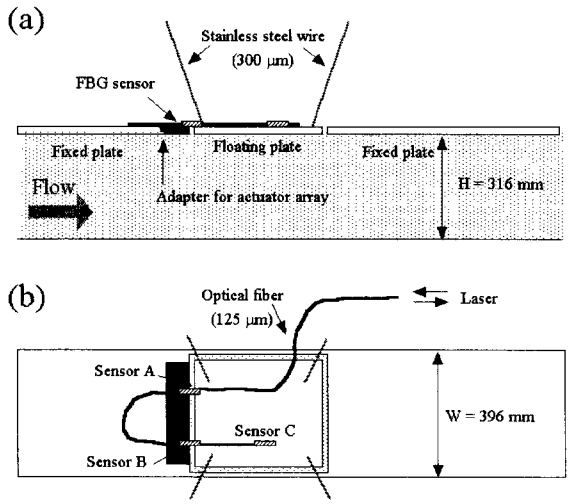

Figure 1: Schematic diagram of FBG system for measuring turbulent skin frictional drag. (a) Side view, (b) top view. Active control devices can be attached in the darker area.

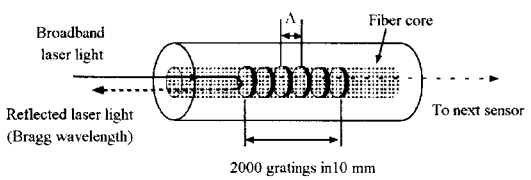

Figure 2: Schematic drawing of fiber Bragg grating sensor.

in the sweep process, higher-speed clusters in a far region rush toward the wall. Such precise understanding provides valuable clues on how to react to or manipulate the local flow events. If we can organize artificial disturbances properly synchronized with the near-wall coherent motions and structures, we may be able to manage the turbulent skin friction drags with greater sophistication. Recently, Segawa et al. (2002) observed the interactions between low-speed coherent structures and artificial disturbances within a fully developed turbulent flow in a closed loop water channel. In their experiment, artificial disturbances were produced by a series of oscillating piezo-ceramic actuators arranged in the spanwise direction. The low-speed structures generated by the actuator array interacted with the longitudinal vortices and inhibited the development of coherent structures in the vicinity of the wall. A number of studies on the active control of laminar and turbulent flows have been carried out experimentally and numerically. In the experimental studies, various MEMS devices were employed (see, for example, Kerho, 2002 and Lee and Goldstein, 2002).

In addition to the development of the control devices,

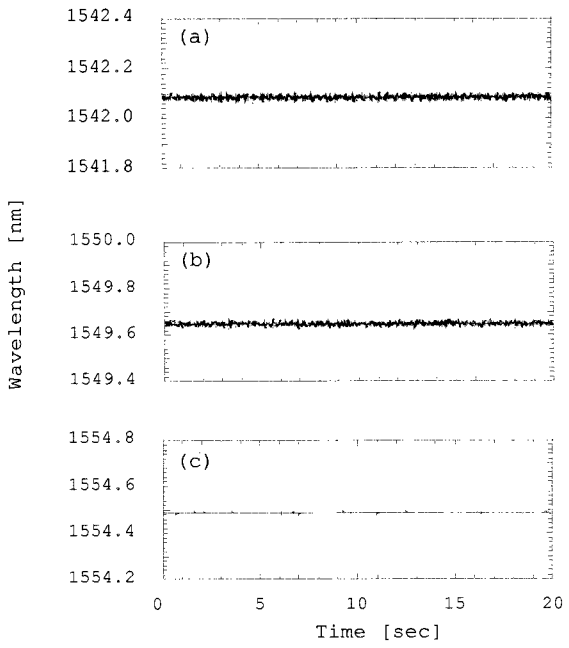

Figure 3: Time series of strain fluctuations measured by FBG system. (a) Sensor A, (b) sensor B, and (c) sensor C.

evaluation of the performances of the devices and the control systems is also important. Specifically, we need to measure the drag variation caused by the actuators. The Preston tube has been widely used to measure skin friction. (see, for example, Hanratty and Campbell, 1983, and Zarbi and Reynolds, 1991). However, the Preston tube method does not have high time response. Thus it is not applicable to flows with higher fluctuation frequencies such as turbulent flows. On the other hand, electrical devices such as load cells and strain gauges are more useful for measuring the high frequency components in the skin friction drag. In spite of the various advantages of load cells and strain gauges, there are still a few disadvantages: they are generally fragile and their output signals are often strongly affected by temperature fluctuations. In addition, adjusting their dynamic range for each experiment is not an easy procedure. Therefore, a more convenient and highly robust drag measurement method with high time resolution is necessary.

In our present study, we developed a new drag measurement technique using a fiber Bragg grating (FBG) system. Using the FBG system we evaluated real-time variations of skin frictional drag induced by several actuators. This is the first attempt to apply an FBG system to fluid dynamic measurements, i.e. an evaluation of the active control of turbulence.

EXPERIMENTAL SETUP

For the purpose of evaluating control devices and control effects, we developed a fiber Bragg grating (FBG) system that can precisely detect minute and tiny strains using a broadband laser. In this study, we verify the applicability of

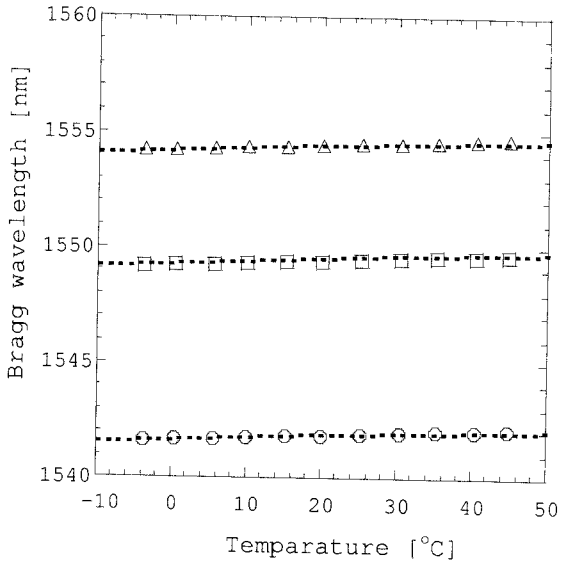

Figure 4: Measured Bragg wavelength shifts of three sensors with temperature changes, A (○), B (□), and C (△). Dotted line shows the fitting by linear function.

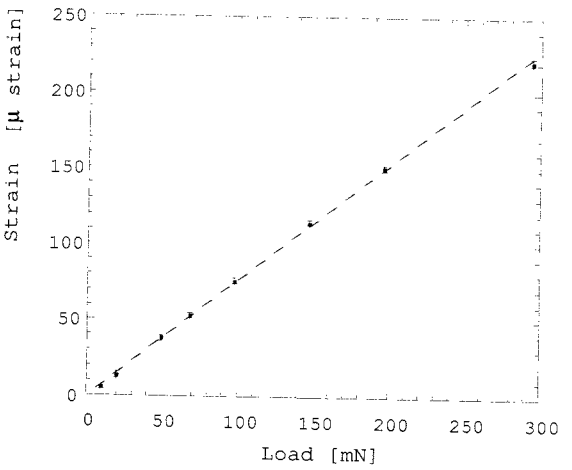

Figure 5: Strain of sensor A as a function of load. Strain fluctuations caused by ambient temperature change were adjusted to the value at 20 °C.

our FBG sensor system for measurements of skin frictional drag and we evaluate the performance of a suction-blowing type actuator array.

The FBG system (NTT, FBG-IS) with three detecting elements (A, B, and C) is shown in Fig. 1. A closed loop water channel with a $1,700 \times 396 \times 315\,\mathrm{mm}^3$ test section was used. The free stream velocity was varied from $U_\infty = 0.1$ to 0.5 m/s. Figure 2 shows a schematic drawing of FBG sensor. The 10 mm long FBG sensor with 2,000 gratings was set at the designed spacing to distinguish it from the other sensors. A broadband laser with a wavelength ranging from 1,528 to 1,568 nm travels through an optical fiber 125 μm in diameter. When the FBG sensor is strained by external forces, the light with the wavelength corresponding to Bragg wavelength (λ_B) is reflected from each sensor following the

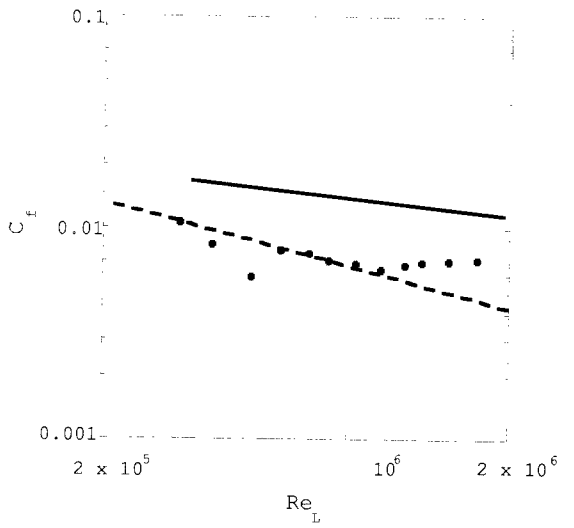

Figure 6: C_f as a function of Reynolds number, $\mathrm{Re}_L = U_\infty(x+L)/\nu$. Dotted and solid lines show $C_f \sim \mathrm{Re}_L^{-1/2}$ and $C_f \sim \mathrm{Re}_L^{-1/5}$ respectively.

relationship:

$$\lambda_B = 2n_0\Lambda, \tag{1}$$

where n_0 is the averaged refractive index in a fiber sensor and Λ is the grating interval. As shown in Fig. 1(b), three sensors are mounted in different locations in a 300 mm long floating flat plate, which is suspended by four stainless steel wires 0.3 mm in diameter and set in the 1,300 mm long steady plate of the channel. Actuator arrays for reactive control of the turbulence are placed upstream of the floating plate, shown as the darker area in Fig. 1. FBG sensors have been widely used for the strain measurement of various structures and elements because of their easily distributed installation (Rao,1999). Figure 3 shows the output signals from the three sensors in Fig. 1(b). In our present study, two detectors, i.e. sensors A and B, were used as strain sensors to precisely measure frictional drag downstream of the actuator array and suspended between the fixed plate and floating plate. The remaining sensor, C, was used to compensate the temperature drift of the FBG system which is extremely sensitive to temperature changes as well as mechanical strain. Figure 4 shows the wavelength shifts of the three sensors in response to temperature changes. In Fig. 4, we find that the sensors stretch 0.01 nm/K. Using sensor C, it is possible to minimize the effect of the temperature drift on the skin frictional drag. Figure 5 shows the strain of sensor A as a function of the load. Strain fluctuations caused by ambient temperature changes were adjusted to the value at 20 °C. As a result, accuracy of the skin friction measurement is improved to as much as 10^{-3} N in our experiment. The dynamic response of our FBG system was found to be higher than 40 Hz.

A wind tunnel with a $2,000 \times 500 \times 1,000\,\mathrm{mm}^3$ test section was used in order to measure the skin friction coefficient of the air for our FBG system. The free stream velocity was variable, ranging from $U_\infty = 2.5$ to 12.5 m/s. The contraction ratio of the duct cross sections was 8:1. The architecture of the measurement system is the same as that of the channel.

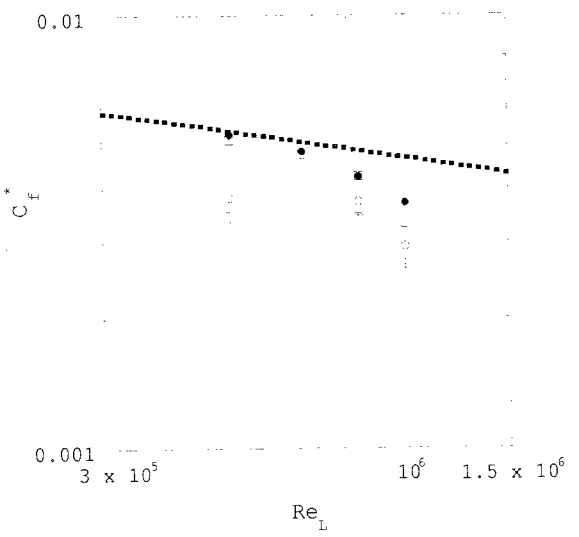

Figure 7: C_f^* vs. Re_L with suction-blowing control in water channel using the FBG system. Dotted line shows $C_f^* = 0.074\mathrm{Re}_L^{-1/5}$. Open symbol (□) indicates C_f^* without suction-blowing. Other open symbols indicate C_f^* with suction-blowing, for $f_p = 1$ Hz (○), 2 Hz (△), and 5 Hz (+). Solid symbol (•) indicates C_f^* without suction-blowing using a load cell.

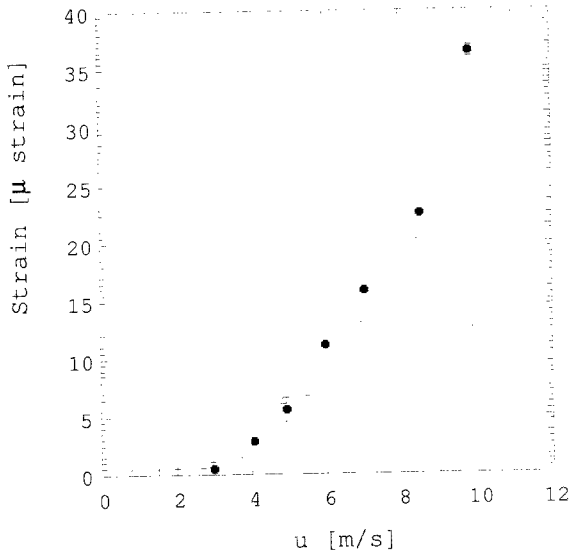

Figure 8: Strain as a function of free stream velocity in wind tunnel. Solid symbol (•) is strain without roughness elements and open symbol (△) is strain without roughness elements.

EXPERIMENTAL RESULTS

Measurement of skin friction drags

The local skin friction coefficient, C_f, in the floating plate in the air and the water was analyzed from data acquired by the FBG sensors. Figure 6 shows C_f as a function of the Reynolds number, $\mathrm{Re}_L = U_\infty(x+L)/\nu$, in the wind tunnel test where x is the distance from the entrance of the tunnel. At a lower Re_L, C_f decreases along the dotted line, which corresponds to $C_f \sim Re_L^{-1/2}$. In this region, the shape factor, H_{12} is 2.6. At higher Re_L, it separates from the line and H_{12} also decreases toward 1.4. Therefore, it was found that the air flow tended to change from a laminar to a turbulent flow.

To compare C_f with the total skin friction coefficient of the entire flat plate in the water channel, we introduced a corrected skin friction coefficient, C_f^*, which is equivalent to the total skin friction coefficient. C_f^* is defined as:

$$C_f^* = (1-\gamma)C_{fL} + \gamma C_{fT}, \tag{2}$$

where γ is the intermittency factor introduced by Dhawan and Narasimha (1958). C_{fL} and C_{fT} are the corrected total skin friction coefficients of the laminar flow and fully developed turbulent flow respectively, which are defined as follows:

$$C_{fL} = \frac{C_f}{\frac{x}{L} + 1 - \left(\left(\frac{x}{L}\right)^2 + \frac{x}{L}\right)^{0.5}}, \tag{3}$$

$$C_{fT} = \frac{C_f}{\frac{x}{L} + 1 - \frac{x}{L}\left(\frac{x}{x+L}\right)^{-0.2}}. \tag{4}$$

In the water channel tests, as can be seen in Fig. 7, C_f^* changes according to $\mathrm{Re}_L^{-1/5}$. This finding implies that the flow exhibited fully developed turbulence over the entire Re_L regime measured in this study. The laminar-turbulent boundary layer transition behavior can be observed using the FBG system.

Drag Variations by Roughness Elements

As a first step in evaluating drag variations caused by the control actuators to be tested, some roughness elements were used in place of the actuators. These roughness elements were 13 balls with 15 mm in diameter. The elements were placed spanwise on the wall at the entrance of the wind tunnel test section. The spacing of the balls was 30 mm. By creating perturbations in the vicinity of the flat plate, the laminar boundary layer tended to change to the turbulent boundary layer. Figure 8 shows strain as a function of the free stream velocity in the wind tunnel. Over the entire range observed, strain increased due to the development of the turbulent boundary layer. The shape factor at the center of the floating plate changed to $H_{12} = 1.4$, when the roughness elements were set on the plate, whereas $H_{12} = 2.6$ without the elements.

Drag Variations by Suction and Blowing

A suction-blowing type actuator array (Fig. 9) was tested as a reactive turbulence control actuator. This actuator can generate horseshoe-like longitudinal vortices by water jets. The array had 40 suction-blowing holes of 1 mm in diameter arranged in the spanwise direction in the stationary plate of the water channel. The water jets are discharged by two separate pistons which are connected to two separate power amplifiers. Suction and blowing are generated alternately by oscillating the two pistons with a phase difference of 180° to each other. Figure 10 shows typical two flow patterns produced by the suction and blowing at a piston frequency of $f_p = 5$ Hz. The horseshoe-like longitudinal vortices are generated by a pair of suction-blowing holes. However, this flow state is unstable and becomes chaotic immediately, as shown in Fig. 10(b). Remarkable changes

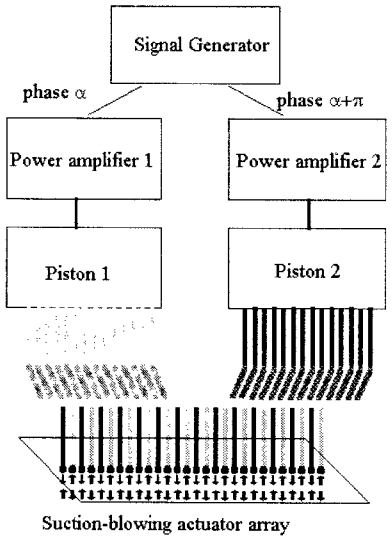

Figure 9: Schematic drawing of suction-blowing actuator jet array. Water jets are discharged by two separate pistons, each connected to a separate power amplifier. Suction and blowing are generated alternately by oscillating two pistons with a phase difference of 180° to each other.

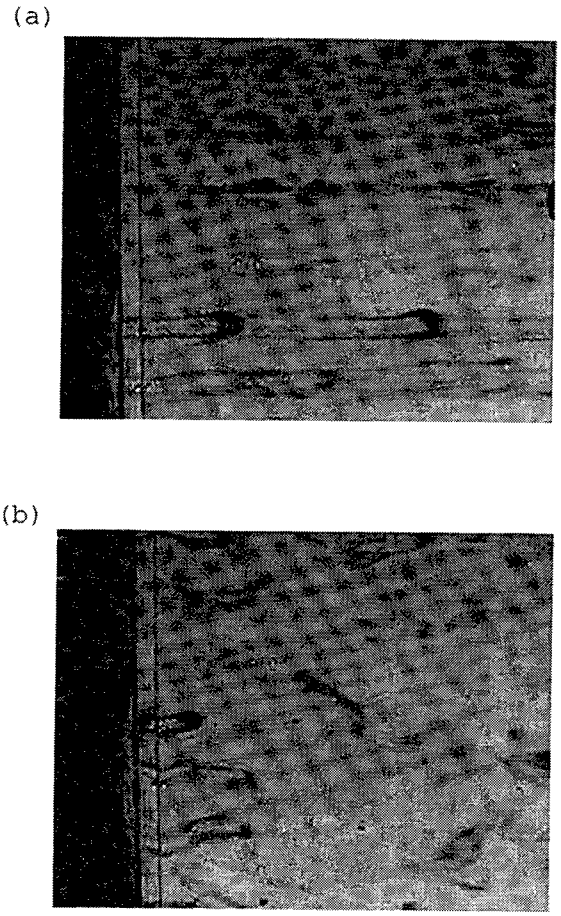

Figure 10: (a) and (b) Two different flow patterns generated by the suction-blowing actuator array driven at the same frequency of $f_p = 5$ Hz.

of the flow pattern caused by the actuator were actually observed. Regarding the drag changes relevant to such flow patterns, we have detected some drag reduction with the suction-blowing control using the FBG system at lower frequencies of the piston, f_p, less than 5 Hz (Fig. 7).

We then considered the mechanism of the drag reduction caused by suction-blowing actuator array. As shown in Fig. 7, C_f^* tends to decrease with the slope of $\mathrm{Re}_L^{-1/5}$ at lower frequencies of the piston, f_p, less than 5 Hz. Downstream of the actuator, horseshoe-like longitudinal vortices were generated from a pair of suction-blowing holes. At a location downstream of the actuator array, clockwise and counter-clockwise longitudinal vortices appear alternatively, as the suction and blowing holes alternated in one half of the suction-blowing period, corresponding to $1/2f_p^{-1}$. It is known that spanwise wall oscillation can generate skin friction reduction in turbulence (for example, see Jung et al., 1992, Laadhari et al, 1994, and Choi et al., 1998a). We supposed that such velocity perturbations might be comparable to the effect of spanwise wall oscillation and lead to reducing the skin friction drags downstream of the suction-blowing actuator array. We also analyzed time series of the strain fluctuations. Figure 11 shows the spectra of the strain fluctuations from the sensors A. We found that there were a typical peak around 3 Hz and it shifted toward higher frequency with the suction blowing control. However, the mechanism of the drag reducing effects is a matter for future study. We are now trying to determine how the suction-blowing actuator affects the near wall flow structure.

In our present study, we examined the feasibility of an FBG system for measuring skin frictional drags. Based on the results shown in Fig. 7, we consider that our FBG system is a promising tool for drag measurements and for use as a flow control sensor. In our next stage of study, we will also use the FBG sensor system to measure various fluid dynamic forces such as airfoil lifts. Application of the FBG system as a separation detector is a challenging topic.

CONCLUDING REMARKS

Throughout all the tests we performed using a wind tunnel and water channel, we considered the FBG system to be a promising tool for precise measurements of minute skin friction variations. We come to this consideration after confirming the following many advantages of the system: 1) Since the FBG sensors are optical, they are hardly influenced by electromagnetic noises; 2) The sequential alignment of the sensors in a single fiber facilitates the signal data processing; 3) The raw output signal of the FBG system exhibited strong linearity against temperature and strain variations, and makes their simultaneous observation possible; 4) The system has a wider dynamic range than conventional methods such as the Preston tube, and finally; 5) The system is very robust in the environment, i.e. durable under higher stresses and applicable for measurements both in air and water. In this study, we showed the feasibility of the FBG system for measurements of frictional drag. In a future study, we will use an FBG sensor system to measure of var-

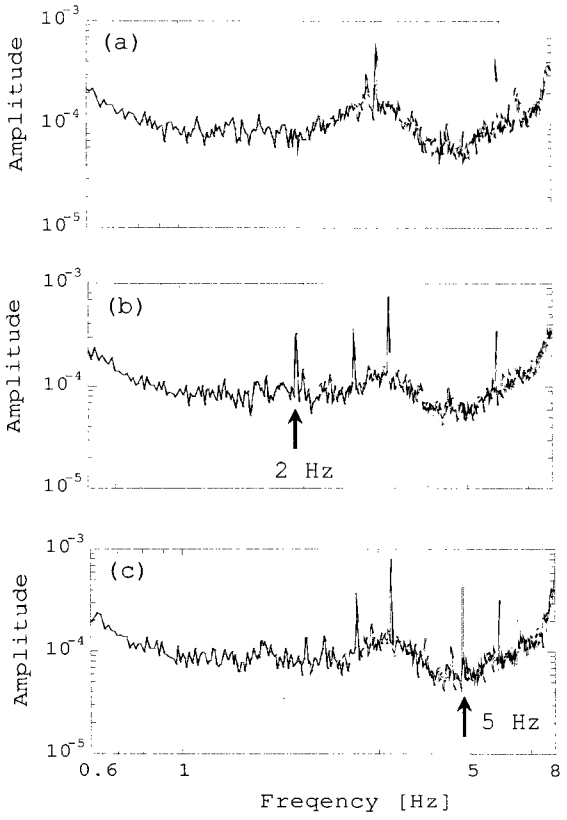

Figure 11: Spectra of time series of strain fluctuation. (a) Without conrol, (b) $f_p = 2\,\mathrm{Hz}$, and (c) $f_p = 5\,\mathrm{Hz}$.

ious fluid dynamic forces, i.e. lift. Application of the FBG system as a separation detector is also considered a promising area of study.

ACKNOWLEDGEMENTS

The authors express their sincere thanks to Prof. M. Ichijo of the Hokkaido University and Dr. Y. Kawaguchi of AIST for their kind advice and stimulating discussions. This research was performed at the Center for Smart Control of Turbulence funded by MECSST of Japan.

REFERENCES

Breuer, K. S., Haritonidis, J. H. and Landahl, M. T., 1989, "The control of transient disturbances in a flat boundary layer through active wall motion" *Physics of Fluids* A, Vol. 1, pp. 574-582.

Choi, K-S., 1989, "Near-wall structure of a turbulent boundary layer with riblets," *Journal of Fluid Mechanics*, Vol. 208, pp. 417-458.

Choi, K-S., DeBisschop, J. R. and Clayton, B. R., 1998a, "Turbulent boundary-layer control by means of spanwise-wall oscillation," *AIAA Journal*, Vol. 36, pp. 1157-1163.

Choi, K-S, and Graham, M., 1998b, "Drag reduction of turbulent pipe flows by circular-wall oscillation," *Physics of Fluids*, Vol. 10, pp. 7-9

Choi, K-S., 2001a, "Turbulent drag-reduction mechanisms: strategies for turbulence management," *Turbulence Structure and Modulation*, A. Soldati and R. Monti, ed., Springer, Wien, CISM Course and Lectures 415, pp. 161-212.

Choi, K-S. and Clayton, B. R., 2001b, "The mechanism of turbulent drag reduction with wall oscillation," *International Journal of Heat and Fluid Flow*, Vol.22, pp. 1-9.

Corino, E. R. and Brodkey, R. S., 1969, "A visual investigation of the wall region turbulent flow," *Journal of Fluid Mechanics*, Vol. 37, pp. 1-30.

Dhawan, S. and Narasimha, R., 1958, "Some properties of boundary layer flow during the transition from laminar to turbulent motion," *Journal of Fluid Mechanics*, Vol. 3, pp. 418-437.

Gad-el-Hak, M, and Blackwelder, R. F., 1989. "Selective suction for controlling bursting events in a boundary layer", *AIAA Journal*, Vol. 27, pp. 308-314.

Gad-el-Hak, M., 2000, *Flow Control: Passive, Active and Reactive Flow Management*, Cambridge University Press, London.

Hanratty, T. J.and Campbell, J. A., 1983, "Measurement of wall shear stress," *Fluid Mechanics Measurements*, R. J. Goldstein, ed., Springer-Verlag, Berlin, pp. 559-615.

Jung, W. J., Mangiavacchi, N. and Akhavan, R., 1992, "Suppression of turbulence in wall-bounded flows by high frequency spanwise oscillations," *Physics of Fluids A*, Vol. 4, pp. 1605-1607.

Kerho, M., 2002, "Active reduction of skin friction drag using low-speed streak control," *AIAA paper*, 2002-0271.

Kimura, M., Tung, S., Lew, J., Ho, C-M., Jiang, F. and Tai, Y-C, 1999, "Measurement of wall shear stress of a turbulent boundary layer using a micro-shear-stress imaging chip," *Fluid Dynamic Research*, Vol. 24, pp. 329-342.

Kline, S. J., Reynolds, W. C., Schraub, F. A. and Runstadler, P. W., 1967, "The structure of turbulent boundary layers," *Journal of Fluid Mechanics*, Vol. 30, pp. 741-773.

Kumar, S. M., Reynolds, W. C. and Kenny, T. W., 1999, "MEMS based transducers for boundary layer control," *Proceedings, 12th IEEE International Conference on Micro Electro Mechanical Systems*, pp. 135-140.

Laadhari, F., Skandaji L. and Morel, R., 1994, "Turbulence reduction in a boundary layer by a local spanwise oscillating surface," *Physics of Fluids A*, Vol. 6, pp. 3218-3220.

Lee, C. Y. and Goldstein, D. B., 2002, "Simulation of MEMS suction and blowing for turbulent boundary layer control," *AIAA paper*, 2002-2831.

Merigaud, E., Anselmet, F., Fulachier, L., Pailhas, G. and Cousteix, J., 1996, "Reduction of parasitic effects related to the turbulent boundary layer on the fuselage using slot suction," *Emerging Techniques in Drag Reduction* K-S. Choi et al., ed., London and Bury St. Edmunds, MEP, pp. 263-280.

Myose, R. Y. and Blackwelder, R. F., 1995, "Control of streamwise vortices using selective suction," *AIAA Journal*, Vol. 33, pp. 1076-1080.

Rao, Y. J., 1999, "Recent progress in applications of in-fibre Bragg grating sensors, *Optics and Lasers in Engineering*, Vol. 31, pp. 297-324.

Segawa, T., Kawaguchi, Y., Kikushima, Y. and Yoshida, H., 2002, "Active control of coherent structures using an actuator array producing inclined wavy disturbances," *Journal of Turbulence*, Vol. 3, 015.

Walsh, M. J. and Lindemann, A. M., 1984, "Optimization and application of riblets for turbulent drag reduction," *AIAA paper*, 84-0347.

Zarbi, G. and Reynolds, A. J., 1991, "Skin friction measurements in turbulent flow by means of Preston tubes," *Fluid Dynamic Research*, Vol. 7, pp. 151-164.